- Cover Page -

Proceedings of the American Society for Composites 18th Technical Conference

Paper Title: Analysis method for inelastic, adhesively bonded joints with anisotropic adherends

Authors: Stanley S. Smeltzer III, NASA Langley Research Center, Eric C. Klang, North Carolina State University

Paper Number: 104

ABSTRACT

A one-dimensional analysis method for evaluating adhesively bonded joints composed of anisotropic adherends and adhesives with nonlinear material behavior is presented in the proposed paper. The strain and resulting stress field in a general, bonded joint overlap are determined by using a variable-step, finite-difference solution algorithm to iteratively solve a system of first-order differential equations. Applied loading is given by a system of combined extensional, bending, and shear forces that are applied to the edge of the joint overlap. Adherends are assumed to behave as linear, cylindrically bent plates using classical laminated plate theory that includes the effects of first-order transverse shear deformation. Using the deformation theory of plasticity and a modified von-Mises yield criterion, inelastic material behavior is modeled in the adhesive layer. Results for the proposed method are verified against previous results from the literature and shown to be in excellent agreement. An additional case that highlights the effects of transverse shear deformation between similar adherends is also presented.

Keywords: joining, anisotropic adherends, adhesive bonding, inelastic yield criterion, shear deformation

INTRODUCTION

Joining metallic and composite structural components with adhesively bonded joints has become a relatively routine and common practice in the technologically advanced aerospace and automotive sectors [1-4]. Finite element methods (FEM) or simple special purpose codes (e.g., one- or two-dimensional analytical methods) are primarily used to obtain the final joint designs in these situations with subsequent verification of the design through testing. The special purpose codes are generally efficient, user-intensive, and lend themselves to conducting parametric studies; however, they are limited to one- or two-dimensional analyses of specific joint configurations. Conversely, FEM are capable of evaluating joints with complex geometry and loading, but are very inefficient for conducting design studies and have serious problems with convergence of analysis results in the regions of interest, i.e. the ends of the joint overlap. The convergence problems are mainly due to the discontinuity in the normal or peel stress at the ends of the overlap, and are manifested by

Stanley S. Smeltzer III, Mechanics and Durability Branch, Mail Stop 190, 8 W. Taylor St., NASA Langley Research Center, Hampton, VA 23681-2199
Eric C. Klang, Mechanical and Aerospace Engineering Department, Box 7910, Raleigh, NC 27695-7910

decreasing the size of the finite element mesh in those regions. The analysis method in the proposed paper was developed to provide efficient tailoring of various joint configurations while incorporating features such as anisotropic adherend behavior, inelastic adhesive behavior, and first-order shear deformation.

The initial characterization of the problems and analysis difficulties associated with an adhesively bonded joint was the classical shear-lag analysis of a single-lap joint by Volkersen [5]. Volkersen identified the incremental deformation of the adherends, but failed to incorporate bending of the adherends that leads to an overall rotation of the joint. This important physical behavior of a single-lap joint was identified in the classical works of both de Bruyne [6] and Goland and Reissner [7]. Specifically, they accounted for the eccentricity that is present between the applied tensile loading in these joints, identified the resulting bending response, and characterized the multi-axial strain state in the adhesive. Additionally, Goland and Reissner further characterized the single-lap joint behavior by formulating a solution for the normal stress perpendicular to the bonded surface in addition to the previously described shear strain. Numerous research studies have been conducted since these classical formulations and much of the early work is found in the excellent reviews by Bensen [8], Sneddon [9], Kutcha [10], and Mathews [11] et al. Of these early works, notable advancements for adhesively bonded joints with composite adherends were made by Erdogan and Ratwani [12], Hart-Smith [13-16], Wah [17], Renton and Vinson [18], and Srinivas [19].

The research performed by Erdogan and Ratwani developed one of the early analytical solutions for a stepped-lap joint configuration, assumed the adherends to be in a state of plane stress, and provided for orthotropic adherend properties. Their solution for the shear stress in an isotropic, elastic adhesive was determined using a strength of materials approach that provided a closed form solution to a system of ordinary differential equations and boundary conditions that were geometry specific. Wah used a similar strength of materials approach for determining the shear and normal stress in a single-lap joint while using classical laminated plate theory to describe the constitutive behavior of the adherends.

Hart-Smith's voluminous works on the behavior of single, double, stepped-lap, and scarf joints have been widely used by the adhesively bonded joint community. His analytical solutions incorporated the effects of adhesive plasticity as well as thermal mismatch and stiffness imbalance between adherends that resulted in efficient codes for performing parametric studies on a wide array of joint configurations. Another important aspect of Hart-Smith's research was the detailed characterization of failure modes in bonded joints with both isotropic and composite adherends.

An important characteristic of adhesively bonded joints with composite adherends is the low transverse stiffness that is often present as a result of the high and ultra-high modulus fibers combined with much lower-modulus polymer resins. Thus, the through-the-thickness properties tend to be dominated by the polymer matrix resulting in a lower transverse stiffness when compared to the in-plane values. Many of the analyses in the early 1970's had incorporated the multi-directional material properties of composite laminates, but had neglected the relatively low transverse stiffness possessed by many of the composite material systems when compared to their isotropic counterparts. Renton and Vinson as well as Srinivas accounted for these low transverse stiffness effects by including first-order shear deformation in their formulations. The method developed by Renton and Vinson was an analytical solution of a single-lap joint geometry that included shear deformation for the composite adherends, and determined the linear elastic response for the adherends and adhesive. Srinivas developed a similar method for single-lap, double-lap, and flush joints that included shear deformation as a part of the analytical solution while attempting to approximate the nonlinear geometric effects.

The more recent works by Bigwood and Crocombe [20,21], Yang [22,23] et al., and Tsai and Morton [24] have made significant advances in the analysis of adhesively bonded joints with composite adherends. Bigwood and Crocombe developed a general joint overlap methodology for evaluating isotropic, adhesively bonded joints with inelastic adhesive behavior and subjected to combined loading. By including inelastic adhesive behavior, significant yielding of the adhesive occurred for

highly loaded joints. This adhesive yielding transferred additional loading to the interior of the adhesive overlap that resulted in a more fully stressed adhesive layer. Yang et al. formulated a method using classical laminated plate theory with first-order shear deformation to analyze symmetric and asymmetric single-lap joints subjected to tensile and bending loading. Tsai and Morton evaluated the three-dimensional strain field present in a tension-loaded, single-lap composite joint.

The current emphasis to develop stiffness tailored wing structures for aircraft applications requires a rapid analysis tool that includes anisotropy of adherends and inelastic adhesive behavior for identification of preliminary bonded joint configurations. The present paper will describe the proposed analysis method for evaluating general, adhesively bonded joint overlaps with anisotropic, shear-deformable adherends and inelastic adhesive behavior that are subjected to combined tensile, shear, and bending moment loading.

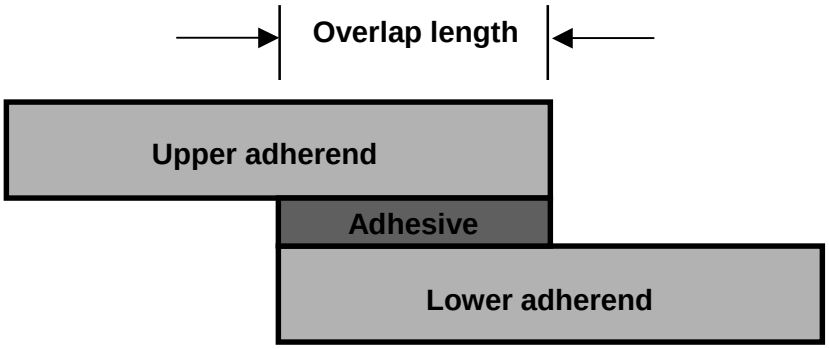

a) A general adhesively bonded joint with a joint overlap

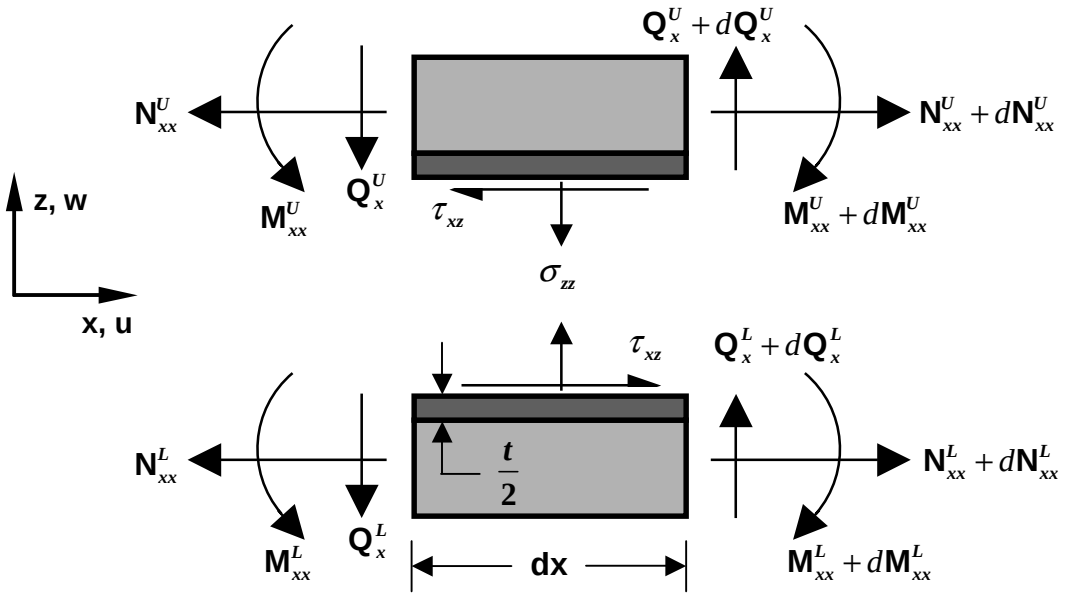

b) Differential element of the joint overlap

Figure 1 Adhesively-bonded joint configuration and element loading.

ANALYTICAL DEVELOPMENT

A description of the basic geometry and a differential element for a joint overlap that is contained within a general adhesively bonded joint is shown in Fig. 1. The adhesively bonded joint is composed of two laminated composite plates, referred to as upper and lower adherends, and an adhesive layer. The adherends are assumed to behave as linear elastic, cylindrically bent plates under a plane strain condition while the adhesive layer is modeled as a nonlinear, isotropic material. Specifically, components of shear and normal stress within the adhesive layer are nonlinear functions of the adhesive strains. Additionally, the effects of transverse shear deformation in the adherends are approximated. This is accomplished by relaxing the requirement from classical plate theory that lines normal to the cross-section remain normal, which is referred to as first-order shear-deformable, laminated plate theory. As a result of the assumption of cylindrical bending, only a cross-section of the entire joint is modeled; therefore, the loading in the figure is given in terms of a unit width joint. Superscript letters, U for the upper adherend and L for the lower adherend, identify variables and loading for each adherend while equivalent terms for the adhesive layer do not have any special notation.

The Euler-Lagrange equations of equilibrium are given in Eqns. (1)-(3) where $\mathbf{N}^i$ represents an

$$\frac{\partial \mathbf{N}_{xx}}{\partial x} + \frac{\partial \mathbf{N}_{xy}}{\partial y} = \mathbf{0} \tag{1}$$

$$\frac{\partial \mathbf{N}_{xy}}{\partial x} + \frac{\partial \mathbf{N}_{yy}}{\partial y} = \mathbf{0} \tag{2}$$

$$\frac{\partial^2 \mathbf{M}_{xx}}{\partial x^2} + 2\frac{\partial^2 \mathbf{M}_{xy}}{\partial x \partial y} + \frac{\partial^2 \mathbf{M}_{yy}}{\partial y^2} + \mathbf{N}^i + q = \mathbf{0} \tag{3}$$

in-plane force term and q is a transverse applied load. The variables $\mathbf{N}_{ij}$ and $\mathbf{M}_{ij}$ are the familiar stress and moment resultants, respectively. Additionally, the displacements u_o, v_o, and w_o are the midplane displacements in the x, y, and z coordinate directions, respectively. The equilibrium equations are used along with the infinitesimal strain tensor, the constitutive relationships for an anisotropic, laminated plate, and the displacement field for a shear-deformable laminated plate to form a kinematic relationship between the forces and moments and the displacements and rotations. The displacement field for a laminate using first-order shear-deformable plate theory is provided in Eqns. (4)-(6) where ϕ_x and ϕ_y correspond to the rotation of a transverse normal about the y and x axes,

$$u(x, y, z) = u_o(x, y) + z\phi_x(x, y) \tag{4}$$

$$v(x, y, z) = v_o(x, y) + z\phi_y(x, y) \tag{5}$$

$$w(x, y, z) = w_o(x, y) \tag{6}$$

respectively. The former displacement field can be used to generate kinematic relations shown in Eqn. (7) using the infinitesimal strain tensor, ε_{ij}, which is written in terms of normal and engineering

$$\begin{Bmatrix} \varepsilon_{xx} \\ \varepsilon_{yy} \\ \gamma_{yz} \\ \gamma_{xz} \\ \gamma_{xy} \end{Bmatrix} = \begin{Bmatrix} u_{o},_{x} \\ v_{o},_{y} \\ w_{o},_{y} + \phi_{y} \\ w_{o},_{x} + \phi_{x} \\ u_{o},_{y} + v_{o},_{x} \end{Bmatrix} + z \begin{Bmatrix} \phi_{x},_{x} \\ \phi_{y},_{y} \\ 0 \\ 0 \\ \phi_{x},_{y} + \phi_{y},_{x} \end{Bmatrix} \tag{7}$$

shear strains. The constitutive relationship for an anisotropic, laminated plate is given in Eqns. (8) and (9), where the $\overline{Q_{ij}}$ terms are referred to as the transformed, reduced-stiffness properties that are derived from the plane stress, reduced- stiffnesses. Components of the stress tensor, σ_{ij}, are written

$$\begin{Bmatrix} \sigma_{xx} \\ \sigma_{yy} \\ \tau_{xy} \end{Bmatrix} = \begin{bmatrix} \overline{Q}_{11} & \overline{Q}_{12} & \overline{Q}_{16} \\ \overline{Q}_{12} & \overline{Q}_{22} & \overline{Q}_{26} \\ \overline{Q}_{16} & \overline{Q}_{26} & \overline{Q}_{66} \end{bmatrix} \cdot \begin{Bmatrix} \varepsilon_{xx} \\ \varepsilon_{yy} \\ \gamma_{xy} \end{Bmatrix} \tag{8}$$

$$\begin{Bmatrix} \sigma_{yz} \\ \sigma_{xz} \end{Bmatrix} = \begin{bmatrix} \overline{Q}_{44} & \overline{Q}_{45} \\ \overline{Q}_{45} & \overline{Q}_{55} \end{bmatrix} \cdot \begin{Bmatrix} \gamma_{yz} \\ \gamma_{xz} \end{Bmatrix} \tag{9}$$

in terms of normal and engineering shear stress. Therefore, Eqns. (4)-(9) are used to form the kinematic relationship given in Eqn. (10) where the ***A***, ***B***, and ***D*** matrices are the common extensional, bending, and extensional-bending coupling stiffness matrices from laminated plate

$$\begin{Bmatrix} \mathbf{N}_{xx} \\ \mathbf{N}_{yy} \\ \mathbf{N}_{xy} \\ \mathbf{M}_{xx} \\ \mathbf{M}_{yy} \\ \mathbf{M}_{xy} \end{Bmatrix} = \left[\begin{array}{c|c} \boldsymbol{A} & \boldsymbol{B} \\ \hline \boldsymbol{B} & \boldsymbol{D} \end{array}\right] \cdot \begin{Bmatrix} u_{o},_{x} \\ v_{o},_{y} \\ u_{o},_{y} + v_{o},_{x} \\ \phi_{x},_{x} \\ \phi_{y},_{y} \\ \phi_{x},_{y} + \phi_{y},_{x} \end{Bmatrix} \tag{10}$$

theory. In addition to the relationship in Eqn. (10), another kinematic relationship is required that relates the transverse shear forces, $\mathbf{Q}_x$ and $\mathbf{Q}_y$, to the strains. This necessary relationship is obtained by integrating Eqn. (9) through the thickness of the laminate using the definition of the transverse shear forces, Eqn. (11), and substituting the displacement field in Eqns. (4)-(6). This provides Eqn.

$$\begin{Bmatrix} \mathbf{Q}_y \\ \mathbf{Q}_x \end{Bmatrix} = \mathbf{K}_s \sum_{k=1}^{N} \int_{z_k}^{z_{k+1}} \begin{Bmatrix} \sigma_{yz} \\ \sigma_{xz} \end{Bmatrix} \cdot dz \tag{11}$$

(12), where A_{44}, A_{45}, and A_{55} are additional extensional stiffness terms and $\mathbf{K}_s$ is a shear correction

$$\begin{Bmatrix} \mathbf{Q}_y \\ \mathbf{Q}_x \end{Bmatrix} = \mathbf{K}_s \begin{bmatrix} A_{44} & A_{45} \\ A_{45} & A_{55} \end{bmatrix} \begin{Bmatrix} w_{o},_{y} + \phi_{y} \\ w_{o},_{x} + \phi_{x} \end{Bmatrix} \tag{12}$$

factor. Although the application of a shear correction factor to the right hand side of Eqn. (11) is traditional, a brief explanation for the use of this factor in the present study is in order.

A well-known fact from elementary beam theory that also applies to plates is that the transverse shear stresses are parabolic in the thickness direction. However, looking back at the earlier described strain field in Eqn. (7), it is evident that the transverse shear strains are represented as constant values through the thickness of the plate. This characterization of the transverse shear strains is a result of assumptions made for the displacement field. Since the transverse shear strains are constant through the thickness of the plate, the resulting shear stresses are also constant. Although there are no provisions within the kinematics of first-order shear-deformable plate theory to remedy the inconsistency between the actual parabolic variation of transverse shear stress and the assumed constant value, the values of the shear forces may be corrected by applying a shear correction factor to the stiffness matrix. This has the result of modifying the transverse shear stiffness of the plate. Additionally, the values for an appropriate shear correction factor can vary with extensional stiffness, Poisson's ratio, transverse shear stiffness, and geometry for a given plate [25-27]. Thus, to perform the analyses in the present study in a uniform manner, a value of one was chosen for the shear correction factor.

Expressions that relate the unit width joint loading and the adhesive stresses are formulated using force and moment equilibrium in the horizontal and vertical directions on each free-body diagram in Fig. 1b. The overlap section is divided at the mid-plane of the adhesive layer, which provides half of the total adhesive thickness along the bottom surface of the upper adherend and half along the upper surface of the lower adherend. Summing forces in the direction of the positive x and z-axes and moments about the y-axis through the mid-plane of each adherend, the state of equilibrium is shown in Eqns. (13)-(15) for the upper adherend where $\boldsymbol{h_U}$ is the upper adherend height and $\boldsymbol{t}$ is the total

$$\sum \mathrm{F_x}: \qquad \mathbf{N}_{xx}^{U} + d\mathbf{N}_{xx}^{U} - \mathbf{N}_{xx}^{U} - \boldsymbol{\tau}_{xz} dx = \mathbf{0} \tag{13}$$

$$\sum \mathrm{F_z}: \qquad \mathbf{Q}_{x}^{U} + d\mathbf{Q}_{x}^{U} - \mathbf{Q}_{x}^{U} - \boldsymbol{\sigma}_{zz} dx = \mathbf{0} \tag{14}$$

$$\sum \mathrm{M_y}: \qquad \begin{aligned} &\mathbf{M}_{xx}^{U} - \left(\mathbf{M}_{xx}^{U} + d\mathbf{M}_{xx}^{U}\right) + \mathbf{Q}_{x}^{U}\left(\frac{dx}{2}\right) + \left(\mathbf{Q}_{x}^{U} + d\mathbf{Q}_{x}^{U}\right) \\ &-\boldsymbol{\tau}_{xz} dx\left(\frac{\boldsymbol{h}_U + \boldsymbol{t}}{2}\right) = \mathbf{0} \end{aligned} \tag{15}$$

adhesive thickness. A similar set of equations is obtained for the lower adherend. The familiar equation for the displacement of a plate in cylindrical bending is used to describe the deflection of the

$$\frac{d^2 w_o^U}{dx^2} = -\frac{A}{D}\mathbf{M}_{xx}^{U} \tag{16}$$

$$\frac{d^2 w_o^L}{dx^2} = -\frac{A}{D}\mathbf{M}_{xx}^{L} \tag{17}$$

where $\boldsymbol{A = A_{11}A_{66} - A_{16}^2}$, $\boldsymbol{B = B_{11}A_{66} - B_{16}A_{16}}$, $\boldsymbol{C = A_{11}B_{16} - A_{16}B_{11}}$ and $\boldsymbol{D = AD_{11} - BB_{11} - CB_{16}}$.

joint overlap for each adherend, and is given by Eqns. (16) and (17). Since the joint overlap is assumed to behave in cylindrical bending, all terms that contain derivatives with respect to y may be neglected. Applying the assumption of cylindrical bending to the kinematic relationship in Eqn. (7), a

$$\begin{Bmatrix} u_{o,x} \\ 0 \\ v_{o,x} \\ -w_{o,xx} \\ 0 \\ 0 \end{Bmatrix} = \left[\begin{array}{c|c} A & B \\ \hline B & D \end{array}\right]^{-1} \cdot \begin{Bmatrix} \mathbf{N}_{xx} \\ \mathbf{N}_{yy} \\ \mathbf{N}_{xy} \\ \mathbf{M}_{xx} \\ \mathbf{M}_{yy} \\ \mathbf{M}_{xy} \end{Bmatrix} \tag{18}$$

reduced form of Eqn. (10) is obtained and inverted to yield Eqn. (18). Using this constitutive equation, a relationship can be determined for the longitudinal and bending normal strain in each adherend. Since the adherends are assumed to behave in cylindrical bending, the loading perpendicular to the joint cross-section is neglected, that is $\mathbf{N}_{yy} = \mathbf{N}_{xy} = \mathbf{M}_{yy} = \mathbf{M}_{xy} = \mathbf{0}$. Thus, the terms for longitudinal and bending normal strain can be determined directly from Eqn. (18) and written as separate equations. Assuming laminate symmetry, the longitudinal and bending normal strain can be combined to form an expression for the total normal strain along the x-axis at the adherend- adhesive interface for each adherend as shown in Eqns. (19) and (20).

$$\varepsilon_{xx}^{U} = \frac{du^{U}}{dx} = \left(A_{11}^{U}\right)^{-1} \mathbf{N}_{xx}^{U} - \frac{h_U}{2}\left(D_{11}^{U}\right)^{-1} \mathbf{M}_{xx}^{U} \tag{19}$$

$$\varepsilon_{xx}^{L} = \frac{du^{L}}{dx} = \left(A_{11}^{L}\right)^{-1} \mathbf{N}_{xx}^{L} + \frac{h_L}{2}\left(D_{11}^{L}\right)^{-1} \mathbf{M}_{xx}^{L} \tag{20}$$

Relationships for the shear and transverse normal strain in the adhesive are provided by Eqns. (21) and (22) in terms of the longitudinal and transverse displacements of the upper and lower

$$\gamma_{xz} = \frac{1}{t}\left(u^{U} - u^{L}\right) \tag{21}$$

$$\varepsilon_{zz} = \frac{1}{t}\left(w^{U} - w^{L}\right) \tag{22}$$

adherends. As a result, the shear and normal strain are assumed to remain constant through the thickness of the adhesive. Additionally, the adhesive is assumed to behave as an isotropic, elastic-plastic material. The plastic material behavior is modeled using the deformation theory of plasticity which provides for quasi-static loading that is applied in increasing proportions, otherwise referred to as proportional loading. Assuming the adhesive remains in a state of plane strain, the constitutive

$$\sigma_{zz} = \frac{E_s \varepsilon_{zz}}{\left(1-\mu_p^2\right)} \tag{23}$$

$$\sigma_{yy} = \frac{E_s \mu_p \varepsilon_{zz}}{\left(1-\mu_p^2\right)} \tag{24}$$

$$\tau_{xz} = \frac{E_s \gamma_{xz}}{2\left(1+\mu_p\right)} \tag{25}$$

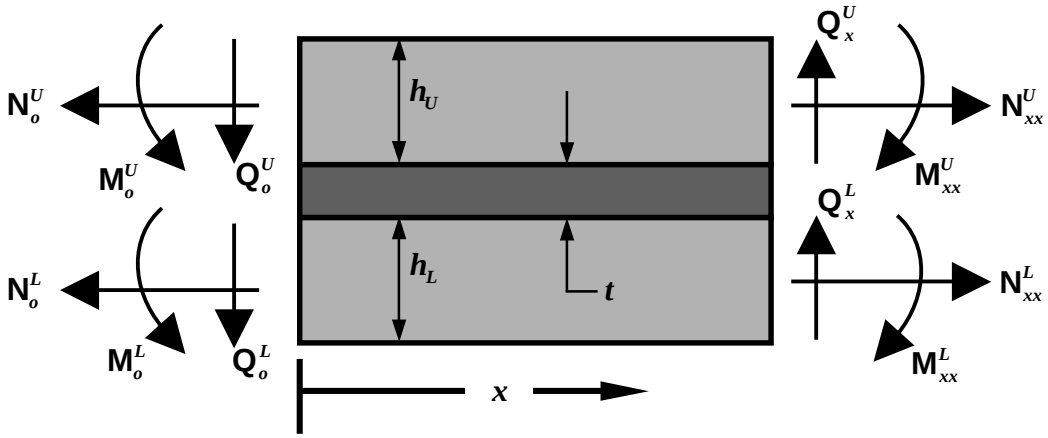

Figure 2 Loading equilibrium for a general section of the bonded joint overlap.

relationships for the adhesive layer are given by Eqns. (23)- (25) where E_s is referred to as the secant modulus and μ_p as the plastic Poisson's ratio. The plastic Poisson's ratio is defined by Eqn. (26) and ranges from an elastic value, μ, to the asymptotic value of 0.5 for the fully plastic case. The secant

$$\mu_p = \frac{1}{2}\left[1 - \frac{E_s}{E}(1-2\mu)\right] \tag{26}$$

modulus, Eqn. (27), is defined by the slope of a line on the uniaxial stress-strain curve taken from the origin to a point along the curve denoted by σ_u and ε_u which are referred to as the equivalent

$$E_s = \frac{\sigma_u}{\varepsilon_u} \tag{27}$$

uniaxial stress and strain, respectively. Finally, by utilizing the equilibrium model of the joint overlap given in Fig. 2 and the previous equations in this section, a system of differential equations is determined and shown in Eqns. (28)-(33) that provides the normal and shear strain along the adhesive layer in terms of the loading and geometry for the upper and lower adherends.

$$N_{xx}^U{}_{,x} = \left[\frac{E_s}{2(1+\mu_p)}\right]\cdot\gamma_{xz} \tag{28}$$

$$Q_x^U{}_{,x} = \left[\frac{E_s}{\left(1-\mu_p^2\right)}\right]\cdot\varepsilon_{zz} \tag{29}$$

$$M_{xx}^U{}_{,x} = Q_x^U - \left[\frac{E_s\left(h_U+t\right)}{4(1+\mu_p)}\right]\cdot\gamma_{xz} \tag{30}$$

$$\frac{dF}{dx} = \frac{1}{t}\left\{\frac{A^L}{D^L}\left[\mathsf{M}_o^U + \mathsf{M}_o^L - \mathsf{M}_{xx}^U + x\left(\mathsf{Q}_o^U + \mathsf{Q}_o^L\right) - h^*\left(\mathsf{N}_{xx}^U - \mathsf{N}_o^U\right)\right] - \frac{A^U}{D^U}\mathsf{M}_{xx}^U\right\} \tag{31}$$

$$\frac{d\varepsilon_{zz}}{dx} = F \tag{32}$$

$$\begin{aligned}\gamma_{xz,x} = \frac{1}{t}\Bigg\{&\mathsf{N}_{xx}^U\left[\left(A_{11}^U\right)^{-1} + \left(A_{11}^L\right)^{-1} + \frac{h^* h_L}{2}\left(D_{11}^L\right)^{-1}\right] - \left(A_{11}^L\right)^{-1}\left(\mathsf{N}_o^U + \mathsf{N}_o^L\right)\\ &- \mathsf{M}_{xx}^U\left[\frac{h_U}{2}\left(D_{11}^U\right)^{-1} - \frac{h_L}{2}\left(D_{11}^L\right)^{-1}\right]\\ &+ \varepsilon_{zz}\left[\frac{E_s}{\left(1-\mu_p^2\right)}\right]\left[\left(\frac{h_U}{2\mathsf{K}^U A_{55}^U}\right) - \left(\frac{h_L}{2\mathsf{K}^L A_{55}^L}\right)\right]\end{aligned} \tag{33}$$

$$\text{where } h^* = t + \left(\frac{h_U + h_L}{2}\right)$$

A description of the adhesive yielding behavior is provided in Eqn. (34) in terms of the equivalent uniaxial strain term, ε_u, using a modified version of the von Mises yield criterion that accounts for

$$\begin{aligned}\varepsilon_u = \frac{1}{2s\left(1-\mu_p^2\right)}\Bigg(&\left(1+\mu_p\right)(s-1)\varepsilon_{zz} + \Big\{\Big[(s-1)^2\left(1+\mu_p\right)^2\\ &+ 4s\left(1-\mu_p+\mu_p^2\right)\Big]\varepsilon_{zz}^2 + 3s\left(1-\mu_p\right)^2\gamma_{xz}^2\Big\}^{0.5}\Bigg)\end{aligned} \tag{34}$$

both the normal and shear components of strain as well as the effects of hydrostatic loading [28]. Using a numerical model for the stress-strain response of a particular adhesive, the level of adhesive yielding is determined along the joint overlap by determining an equivalent uniaxial strain from the computed strain field and comparing that to an adhesive yield stress. Therefore, by using Eqns. (28)-(34) the complete elastic-plastic strain field in the adhesive layer is determined in an iterative manner for a given joint loading and geometry configuration.

SINGLE-LAP JOINT MODELS

All the analyses performed for this study evaluated single-lap type joints with adherend and adhesive properties given in Tables 1 and 2. The description of the basic geometry and nomenclature for a single-lap joint was given in Fig. 1. The choice of lamina properties for the upper and lower adherends in the quasi-isotropic model was made in order to simulate average laminate properties that corresponded to those for the isotropic model given in Table 2. The in-plane average laminate properties that correspond to the $[0,45,-45,90]_s$ stacking sequence using the lamina properties in Table 2 are $E_1 = E_2 = 69.5E03$ N/mm^2 and a $\nu = 0.29$. The loading for each of the analyses was a uniform tensile load of 400 Newtons, which corresponds to an end joint loading per unit plate width of $\mathsf{N}_U^o = 400$ N/mm, $\mathsf{Q}_U^o = -24.7$ N/mm, and $\mathsf{M}_U^o = -255.8$ N-mm/mm.

Table 1 Geometry of the single-lap joint models for cases A, B, and C.

Upper adherend thickness, h_U (mm)	2.0
Lower adherend thickness, h_L (mm)	2.0
Adhesive thickness, t (mm)	0.05
Overlap length, L_j (mm)	12.5

Table 2 Material properties for the components of the single-lap joint models in cases A, B, and C.

Lamina Property[a]	Quasi-isotropic Model			Isotropic Model		
	Upper Adherend	Lower Adherend	Adhesive	Upper Adherend	Lower Adherend	Adhesive
E_1, (N/mm^2)	162,000	162,000	1,875	70,000	70,000	1,875
E_2, (N/mm^2)	19,300	19,300	1,875	70,000	70,000	1,875
ν_{12}	0.31	0.31	0.4	0.3	0.3	0.4
G_{12}, (N/mm^2)	11,000	11,000	-	-	-	-
Laminate stacking sequence	$[0,45,-45,90]_s$	$[0,45,-45,90]_s$	-	-	-	-
Yield stress (N/mm^2)	-	-	40.0	-	-	40.0

[a]Subscripts 1 and 2 denote the longitudinal (fiber) and transverse (matrix) directions of an anisotropic lamina, respectively.

Three basic evaluations were conducted of the single-lap joint configuration using the anisotropic, inelastic-adhesive analysis method developed in this paper. The first evaluation, case A, was performed to compare the results of the present analysis method against those of the classical Goland and Reissner closed-form solution. Since the analysis method by Goland and Reissner assumes linear elastic adhesive behavior, the corresponding analysis using the proposed anisotropic, inelastic-adhesive analysis method was performed without considering adhesive yielding. The analysis method by Bigwood and Crocombe that was developed for isotropic adherends was used to verify the inelastic capabilities of the current method in case B. A modified von Mises yield criteria, given in Eqn. (34), was used to evaluate the degradation of the adhesive. The value of *s* used in this study was 1.3, which Raghava et al. determined to be applicable for polymer-type materials. Additionally, a hyperbolic-tangent approximation of the uniaxial stress-strain response used by Bigwood and Crocombe was duplicated for comparison purposes and is restated in Eqn. (35) where the asymptotic

$$\sigma = \mathrm{A}\tanh\left[\frac{\varepsilon \mathrm{E}_s}{\mathrm{A}}\right] \tag{35}$$

stress value, A, is 69.3 N/mm^2. Each of the single-lap joint models analyzed for cases A and B consist of identical upper and lower adherends that are quasi-isotropic.

The last evaluation, case C, was performed to highlight the effect of differences in the transverse shear moduli between the upper and lower adherends. Material properties for the upper and lower adherends for both the baseline and the modified are as previously shown in Table 2 with the exception of the transverse shear modulus. In the analysis of the baseline joint configuration, the value of the transverse shear modulus, G_{13}, is 3.45E03 N/mm^2 for both the upper and lower adherends. In the analysis of the modified joint configuration, the same transverse shear modulus is used for the upper adherend while the value for the lower adherend is increased by 30% to 4.5E03 N/mm^2. The analyses conducted in case C included the nonlinear material behavior for the adhesive in addition to the shear-deformable adherend behavior.

NUMERICAL RESULTS

Analytically predicted results of the single-lap, adhesively bonded joints considered in this study are presented in this section. A Fortran 95 code was written to solve the system of first-order differential equations given in Eqns. (28)-(33) using a variable-step, finite-difference solution algorithm developed by IMSL. Using the author-developed Fortran code and IMSL routine, all of the joint models were analyzed in less than five seconds using a laptop personal computer with an 800 mhz micro-processor and 128 megabytes of RAM.

The shear and normal stress response for the models analyzed in case A are shown in Fig. 3. As discussed earlier, these models were used to compare the results of the present analysis method against those of the classical Goland and Reissner closed-form solution. The results from the present analysis are displayed using a solid curve and stress terms with a superscript *A* while the results for the classical analysis of Goland and Reissner are displayed as dashed curves and stress terms using a superscript *GR*. Excellent agreement between the present analysis method and the classical method by Goland and Reissner is seen for almost the entire elastic shear stress field in 3a and the elastic normal stress field in 3b. The largest deviation between the two methods is found at the location of the peak shear stress on the ends of the joint overlap. An approximately 15% lower peak shear stress is predicted by the present analysis method compared to that of Goland and Reissner. This difference is most likely due to the tendency of the analysis method developed by Goland and Reissner to be conservative for most cases as a result of approximations made during the formation of their solution. These approximations are well documented [29,30] and are a result of neglecting higher-order terms within the differential equations of equilibrium as well as simplifications made to certain mathematical expressions. One other possibility for the peak shear stress difference is a slight discrepancy between the in-plane stiffness for the adherends in the anisotropic and isotropic joint models. As discussed in the previous section, the in-plane average laminate properties that result from the quasi-isotropic stacking sequence using the lamina properties in Table 2 are $E_1 = E_2 =$ 69.5E03 N/mm^2 and a $\nu = 0.29$. Although the plate (laminate) properties for each of the models are very close to the same value, the lamina properties and stacking sequence chosen for the anisotropic analysis provided a slightly more compliant joint. As a result, the peak shearing stress determined from the quasi-isotropic model would tend to be lower than that for the isotropic model.

The strain and resulting stress response for the second bonded joint evaluation, case B, are presented in Figs. 4a and 4b, respectively. Again, as previously discussed, these models were used to compare the present analysis method against the isotropic, elastic-plastic analysis method by Bigwood and Crocombe. The results for the present method are shown by the solid curves in each figure while the isotropic analysis results are displayed as dashed curves. For this case, stresses and strains from the anisotropic analysis are denoted by terms with a superscript *A* while the isotropic

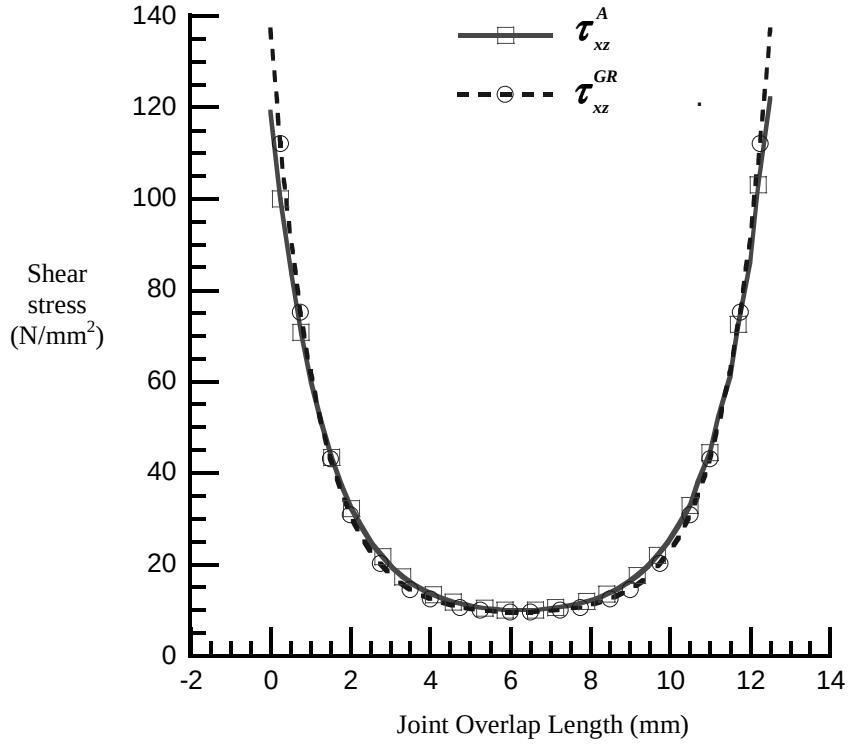

a) Elastic shear stress

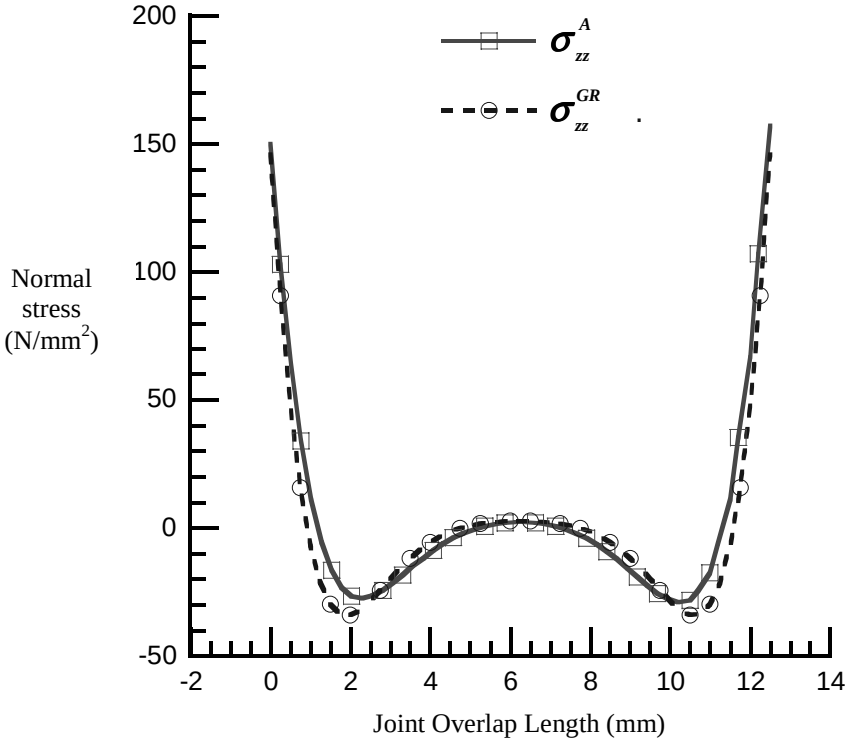

b) Elastic normal stress

Figure 3 Comparison of the anisotropic adhesively bonded joint solution and method by Goland and Reissner [7], case A.

analysis is denoted by terms with a superscript *I*. The joint geometry for the models used in both the isotropic and anisotropic analyses is identical as shown in Table 1. However, as noted in case A, a slight variation is seen between the isotropic adherend properties and the quasi-isotropic laminate properties. In Fig. 4a, a very good agreement is provided between the anisotropic and isotropic solutions with a reduction in shear and normal strain from the isotropic to the anisotropic solutions seen as the solution moves from the center of the overlap towards the joint edges. Since the greatest shear and normal strain are seen at the joint edges, the solution is much more sensitive to changes at those locations. Therefore, the more compliant behavior of the quasi-isotropic adherends causes a reduction in shear and normal stress similar to case A, but to a greater degree due to the inelastic solution. One additional point to note in Fig. 4b is the small drop in the shear stress at the four and eight millimeter points along the joint overlap. This represents the interface between the elastic and the plastic zones in the adhesive layer. Although the solution is continuous for the entire overlap as evident by the curves for the strain in Fig. 4a, the calculation for the degraded material properties results in a sharp decrease at the elastic-plastic zone interface. This is only a very localized effect and is generally located well away from the peak stress regions.

A much more significant reduction in peak shear and normal stress is obtained between the inelastic solution in case B and the elastic solution from case A of the same joint configuration. The peak shear stress for the elastic solution in Fig. 3a was approximately 120 N/mm^2 while the peak shear stress for the inelastic solution in Fig. 4b was approximately 44 N/mm^2, which corresponds to a 67 % reduction. Similarly for the normal stress, a reduction of 67% exists between the 150 N/mm^2 elastic value and the 50 N/mm^2 inelastic value. This significant reduction in adhesive stresses is not obtained without a cost as only a few millimeters of the joint overlap are now stressed below 20 N/mm^2 compared to almost eight millimeters in the elastic joint. Although a much more efficient joint may be obtained by allowing a certain portion of the joint to yield, an important note of caution is prudent for joints that are intended for long-term use, multiple cycles, or hazardous environments. Joints that are intended for these uses may still be designed by taking into account the inelastic adhesive behavior; however, it is crucial that a section of the center of the joint overlap remain well below the yield stress level to serve as an elastic reserve. The need to provide a reasonably long, lightly loaded elastic trough at the center of fatigue joints was first discussed in detail by Hart-Smith [16].

The results for the last case, case C, involved changes between the transverse shear stiffness for the upper and lower adherends, as previously described, and are given in Fig. 5. The results for the baseline analysis are displayed using solid curves and denoted by terms with a superscript *B* while the modified analysis results are displayed as dashed curves and denoted by terms with a superscript *M*. A noticeable difference between the baseline and modified shear strain are readily apparent in Fig. 5a. As the load transfers from the upper adherend to the lower adherend on the left end of the joint overlap, the stiffer, lower adherend forces additional adhesive shearing at the edge, but decreases more rapidly compared to the baseline joint as the solution moves inboard. A reverse of this trend is seen on the right end of the joint overlap as the peak shear stress is reduced for the modified joint; however, a greater degree of straining occurs between the eight and twelve millimeter joint stations. Additionally, the entire solution has shifted towards the left end of the joint overlap and taken on a more asymmetrical appearance. As for the normal strain, little or no change in the solution was obtained between the two joints.

The plot of the shear stress for case C is given in Fig. 5b and reveals several interesting trends. As in case B, the transition zone between the elastic and plastic zones is clearly seen around the four and eight millimeter joint stations. From the figure it appears that an increase in joint stiffness resulted in a small lengthening of the transition zone between the elastic and plastic regions. The peak shear stress is obtained at the ten-millimeter joint station as the load transfers from the stiffer, lower adherend to the more compliant, upper adherend. The peak shear stress at this point is approximately 45 N/mm^2 while the peak shear stress for the left hand portion of the joint is approximately 41 N/mm^2 at the two-millimeter joint station. This amounts to a 9% difference between joint ends with a 7%

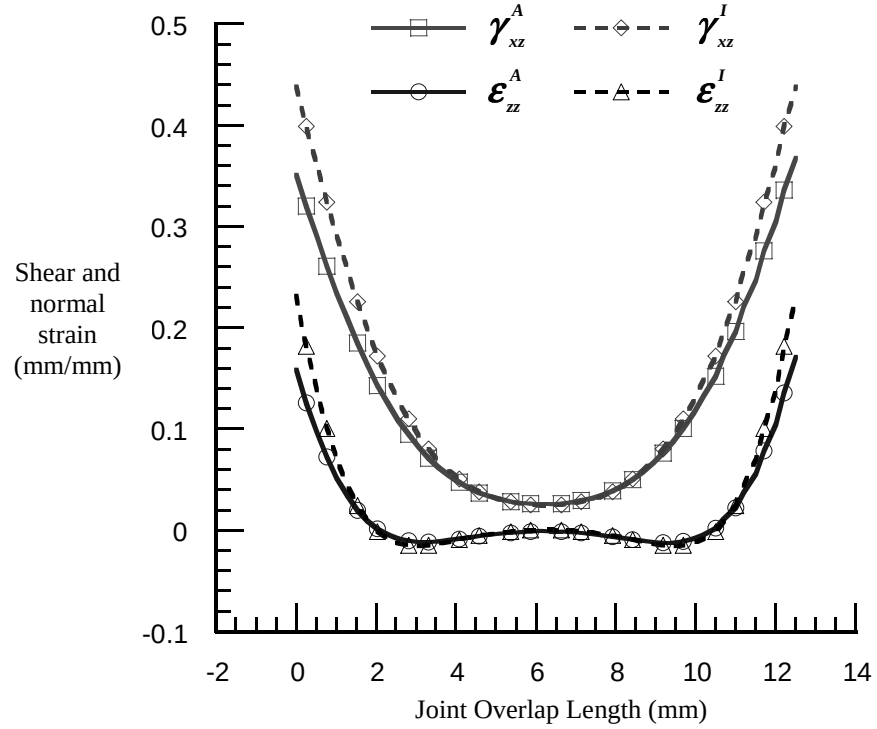

a) Inelastic shear and normal strain

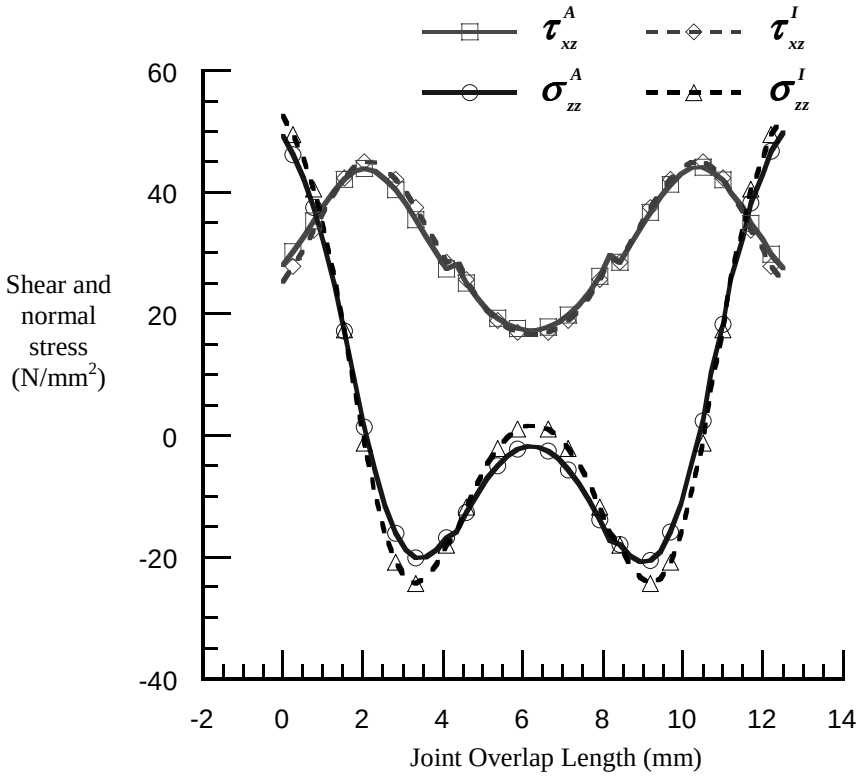

b) Inelastic shear and normal stress

Figure 4 Comparison of the anisotropic adhesively bonded joint solution and method by Bigwood and Crocombe [21], case B.

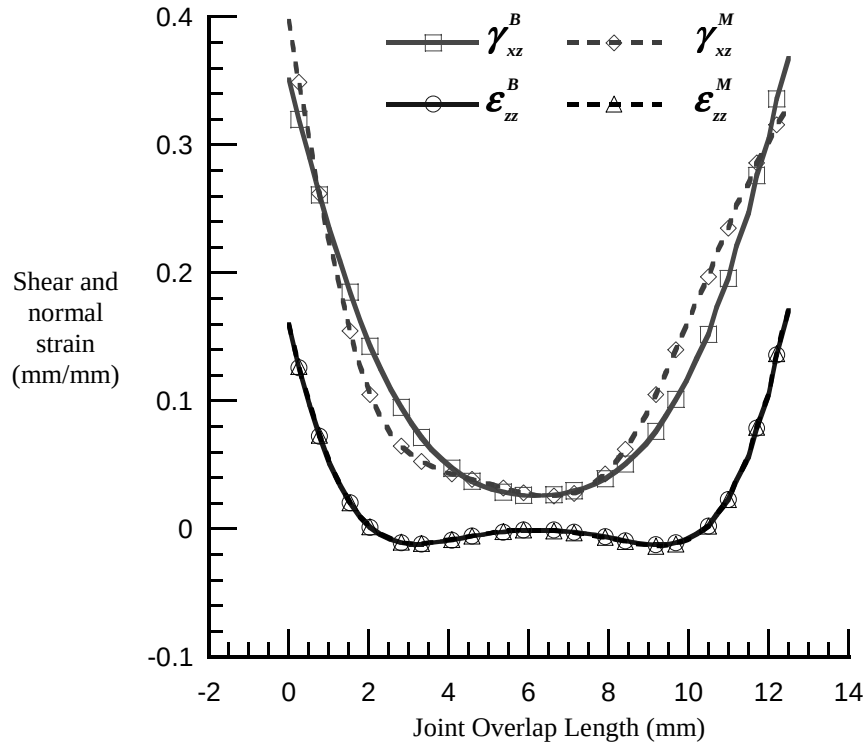

a) Inelastic shear and normal strain

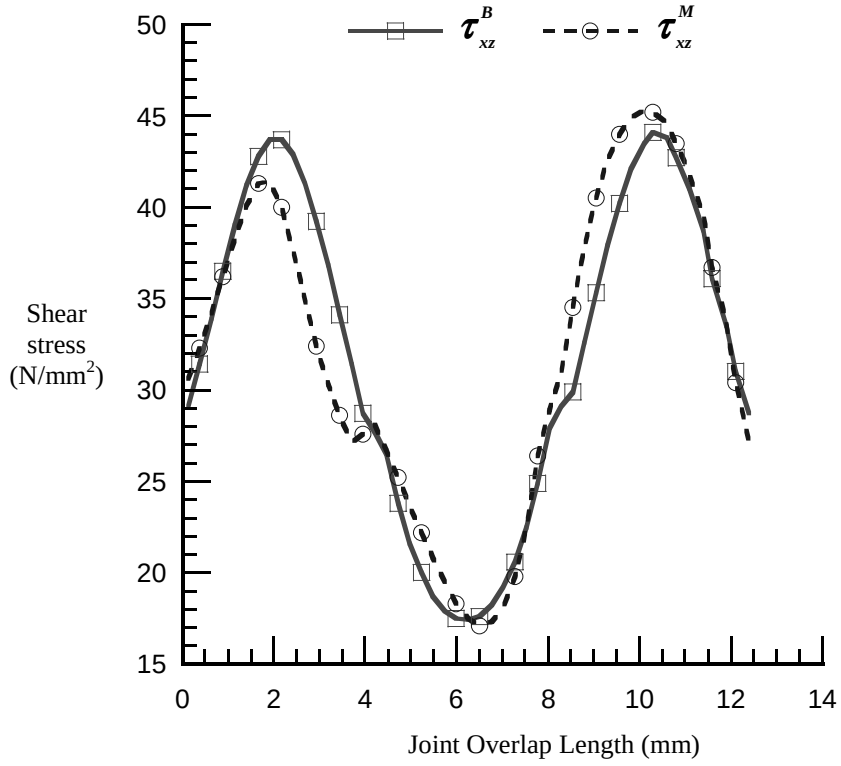

b) Inelastic shear stress

Figure 5 Effect of 30% increase in transverse shear modulus on the strain and stress response for the adhesively bonded joint in case C.

decrease and a 2.5% increase over the baseline solution for the left and right ends of the joint overlap, respectively. Thus, by modifying only the transverse shear stiffness between the upper and lower adherends a drop in the shear stress was obtained at one end of the joint overlap while incurring a slight increase at the opposite end. A joint design utilizing this type of tailored stiffness approach might be applicable to the transition region of an aircraft skin to a longitudinal stiffener where different laminate stiffenesses might be required.

CONCLUDING REMARKS

A new method for evaluating general, adhesively bonded joint overlaps with anisotropic, shear-deformable adherends and inelastic adhesive behavior that are subjected to combined tensile, shear, and bending moment loading was presented. Rapid solution of a wide variety of joint configurations is possible with the Fortran code developed from the proposed theory using a finite-difference solution algorithm. Thus, a tool has been developed that is capable of tailoring the stiffness of the composite adherends in an adhesively bonded joint. Additionally, efficient joint designs are obtained by allowing adhesive yielding that can lead to significantly decreased peak shear and normal stress in the adhesive.

The results of the proposed method were verified using two single-lap joint configurations with isotropic adherends from the literature. Reductions in the peak shear and normal stresses in the adhesive layer of approximately 67% were obtained from the elastic to the inelastic solutions. An additional case was presented that showed the effect of varying the transverse shear stiffness between the upper and lower adherends for quasi-isotropic laminate stacking sequences. Using the varying transverse shear stiffness joint in case C, the potential for tailoring the joint stiffness was demonstrated as a 30% increase in the lower adherend transverse stiffness resulted in a 7% decrease at one end of the joint overlap and a 2.5% increase at the opposite end.

REFERENCES

1. Hart-Smith, L.J., “Adhesive bonding of aircraft primary structures,” *SAE Aerospace Congress and Exposition*, Los Angeles Convention Center, October 1980, pp. 1-15.
2. van Straalen, I.J.J., Wardenier, J., Vogelesang, L.B., and Soetens, F., “Structural adhesive bonded joints in engineering – drafting design rules,” *Int. J. Adhesion and Adhesives*, Vol. 18, 1998, pp. 41-49.
3. Kim, Y.G., Oh, J.H., and Lee, D.G., "Strength of Adhesively-Bonded Tubular Single Lap Carbon/Epoxy Composite-Steel Joints," *J. of Composite Materials*, Vol. 33, No. 20, 1999, pp. 1897.
4. Krueger, R., Cvitkovich, M.K., O’Brien, T.K., and Minguet, P.J., “Testing and Analysis of Composite Skin/Stringer Debonding Under Multi-Axial Loading,” *J. of Composite Materials*, Vol. 34, No. 15, 2000, pp. 1263-1300.
5. Volkersen, V.O., "Die Nietkraftverteilung in zugbeanspruchten Nietverbindungen mit konstanten Laschenquerschnitten," *Luftfahrforschung*, Vol. 15, 1938, pp. 41-47.
6. de Bruyne, N.A., "The Strength of Glued Joints," *Aircraft Engineering*, April 1944, pp. 115-118.
7. Goland, M., and Reissner, E., "The Stresses in Cemented Joints," *J. of Applied Mechanics*, Vol. 66, March 1944, pp. A-18-27.
8. Benson, N.K., “The mechanics of adhesive bonding,” *Applied Mechanics Review*, Vol. 14, No. 2, 1961, pp. 83-87.
9. Sneddon, I.S., “Chapter IX - The Distribution of Stress in Adhesive Joints,” *Adhesion*, Eley, D.D., Ed., Oxford University Press, 1961, pp 207-253.
10. Kutcha, D., "Mechanics of Adhesive Bonded Lap-Type Joints: Survey and Review," Technical Report AFML-TDR-64-298, U.S. Air Force, December 1964.
11. Matthews, F.L., Kilty, P.F., and Godwin, E.W., “A review of the strength of joints in fibre-reinforced plastics – Part 2. Adhesively bonded joints,” *Composites*, January 1982, pp. 29-37.
12. Erdogan, F. and Ratwani, M., “Stress distribution in bonded joints,” *J. of Composite Materials*, Vol. 5, 1971, pp. 378-393.
13. Hart-Smith, L.J., “Adhesive-bonded double-lap joints,” NASA CR-112235, January 1973.
14. Hart-Smith, L.J., “Adhesive-bonded single-lap joints,” NASA CR-112236, January 1973.

15. Hart-Smith, L.J., “Adhesive-bonded scarf and stepped-lap joints,” NASA CR-112237, January 1973.
16. Hart-Smith, L.J., “Non-classical adhesive-bonded joints in practical aerospace construction,” NASA CR-112238, January 1973.
17. Wah T., “Stress distribution in a bonded anisotropic lap joint,” *J. of Engng. Mater. and Tech.*, 1973, pp. 174-181.
18. Renton, W.J. and Vinson, J.R., “The analysis and design of composite material bonded joints under static and fatigue loading,” AFOSR Report 73-1627, 1973.
19. Srinivas, S., “Analysis of bonded joints,” NASA TN D-7855, April 1975.
20. Bigwood, D.A. and Crocombe, A.D., “Elastic analysis and engineering design formulae for bonded joints,” *Int. J. Adhesion and Adhesives*, Vol. 9 No. 4, 1989, pp. 229-242.
21. Bigwood, D.A. and Crocombe, A.D., “Non-linear adhesive bonded joint design analyses,” *Int. J. Adhesion and Adhesives*, Vol. 10, No. 1, 1990, pp. 31-41.
22. Yang, C., Pang, S.S., and Griffin, A.S., “Strength Model of Adhesive-Bonded Double-Lap Joints Under Cantilevered Bending,” *Polymer Engineering and Science*, Vol. 32, No. 9, 1992, pp. 632-640.
23. Yang, C. and Pang, S.S., “Stress-strain analysis of adhesive-bonded single-lap composite joints under cylindrical bending,” *Composites Engineering*, Vol. 3, No. 11, 1993, pp. 1051-1063.
24. Tsai, M.Y. and Morton, J., “Three dimensional deformation in a single-lap joint,” *J. of Strain Analysis*, Vol. 29, No. 1, 1994, pp. 137-145.
25. Reissner, E., “The effect of transverse shear deformation on the bending of elastic plates,” *ASME J. of Applied Mechanics*, Vol. 12, 1945, pp. A69-77.
26. Bert, C.W. and Gordaninejad, F., “Transverse shear effects in bimodulur composite laminates,” *J. of Composite Materials*, Vol. 17, 1983, pp. 282-298.
27. Wittrick, W.H., “Analytical, three-dimensional elasticity solutions to some plate problems, and some observations on Mindlin’s plate theory,” *Int. J. of Solids and Structures*, Vol. 23, 1987, pp. 441-464.
28. Raghava, R., Caddell, R.M., and Yeh G.S.Y., “The macroscopic yield behavior of polymers,” *J. of Material Science*, Vol. 8, 1973, pp. 225-232.
29. Allman, D.J., “A theory for elastic stresses in adhesive bonded lap joints,” *Quarterly J. of Mechanics and Applied Mathematics*, Vol. 30, No.4, 1977, pp. 415-436.
30. Cooper, P.A. and Sawyer, J.W., “A Critical Examination of Stresses in an Elastic Single Lap Joint,” NASA TP-1507, 1979.